Color image analysis of quaternion discrete radial Krawtchouk moments

Hicham Amakdouf[1] · Amal Zouhri[1] · Mostafa EL Mallahi[1,2] · Hassan Qjidaa[1]

Abstract

In this work, we suggest a new set of quaternion discrete radial Krawtchouk moments (QDRKMs) for color image reconstruction and classification. These new discrete moments are represented over a disk by using discrete orthogonal radial Krawtchouk moments. The use of Quaternion discrete moments for color image eliminates the discretization errors produced when the Quaternion continuous moments are used. Furthermore, this approach is suggested for highly accurate calculation of QDRKMs in polar coordinates where the kernel is exactly calculated by over circular color pixels. The translation, scaling, and rotation (TSR) invariances for QDRKMs are proved. Theoretical analysis and numerical experiments investigation were shown in terms of the performance description of TSR invariances, classification and robustness to different noises of the QDRKMs compared with continuous quaternion Legendre–Fourier moments using COIL 100 database.

Keywords Color image analysis; quaternion · Discrete radial Krawtchouk moments · Classification and recognition of color image

---

✉ Hicham Amakdouf
   Hicham.amakdouf@usmba.ac.ma

   Amal Zouhri
   amal.zouhri@usmba.ac.ma

   Mostafa EL Mallahi
   mostafa.elmallahi@usmba.ac.ma

   Hassan Qjidaa
   hassan.qjidaa@usmba.ac.ma

[1] Sidi Mohamed Ben Abdellah University, Faculty of Sciences Dhar el Mahraz, Fez, Morocco

[2] Sidi Mohamed Ben Abdellah University, Laboratory of Computer Science and Interdisciplinary Physics, ENS, Fez, Morocco

1 Introduction

In recent years, and with the fast progress of mathematics, computer science, and technological development of digital cameras, almost of the images are chromatic. Indeed, to transmit or stock more information, the digital color images have more potential than a gray level or binary image. Moreover, the values associated of three colors such as green, blue, and red for each level of the pixel or and as well its hue, brightness, and saturation, can be successful when used in many images processing tasks such as reconstruction, object classification, recognition, registration, and segmentation.

The traditional approach to treatment with digital color images has each level separate while processing, employing a gray level method, and to combining the individual output results. As a consequently, this method misses the inherent correlation between the entities of three colors level. The main problem is therefore to handle three values of each pixel level in entirety.

To solve this problem, recently, algebra quaternion color image analysis to represent digital color images by encoding three levels into the imaginary parts by B. J. Chen et al. [4]. The performance of this quaternion algebra is widely seen when a digital color image is treated as a vector space. Firstly, the quaternion algebra is exploited in digital color image processing for the continuous moments by Chen et al. [3], as well as, [5] using the color image representations by the quaternion type moment functions. Moreover, and to ensure the rotation invariance in the problems of classification; researchers introduced continuous radial moments. Indeed, Xiao [25] came up with the radial moments of Legendre, and extended them in 3D case by El Mallahi et al. [16]. The quaternion pseudo-Zernike moments their RST invariants are defined by Chen et al. [6]. They used these continuous moments in color image recognition. The quaternion radial Fourier moments for digital color image processing are defined by Xiang-Yang et al. [23]. The quaternion polar complex moments of TRS invariants for digital color image representation defined by Wang et al. [22]. Unfortunately, their methods for computing quaternion continuous moments are limited by the discretization error, the high computational cost and the propagation of a numerical error in the computation of continuous polynomials values [7, 8].

These methods result problems of redundancy, and discretization due to finding out errors caused by numerical estimation of integrals in the computation of continuous moments. Indeed, the computation of orthogonal continuous moments requires appropriate transformations of the coordinates of image representation in the interval of definition of the continuous polynomials along with, the calculation of the integral using the finite summations. But, this transformation causes an error of discretization. So as to solve that issue for the gray level images, scientists suggested some methods based on the discrete moments using a discrete polynomials such as the ones of Krawtchouk [2, 9, 11–13, 26] Tchebitchef's [14–16, 24], Meixner's [14], Charlier's [1, 15], Hahn's [10, 19–21], dual Hahn's [17, 20], and Racah's [18] for image processing. The calculation of discrete moments eliminates the need for numerical approximation and satisfies exactly the orthogonality property in discrete space coordinates of the image.

For conserving the color image, no work has been suggested to solve the problem. In this work, and in order to solve this problem of the color image, we opt for an exact method to eliminate the discretization errors and preserve the invariant to the rotation. This method is based on discrete radial moments and classification using multilayer perceptron [1]. We them, we suggest two contributions.

We first introduce a new method for computing an exact, stable and fast computation of higher order QDRKMs in circular coordinates. In this contribution, the use of a discrete form of the Radial Tchebichef polynomials has removed the discretization error granting a height stabilization of the aforementioned method.

Second, we put a new method for extracting translation, scaling and rotation invariants of QDRKMs. The experimental results show highly accurate color image reconstruction of the proposed approach.

These new discrete moments are represented over a disk by using discrete orthogonal radial Krawtchouk moments. The use of discrete moments eliminates the discretization errors produced when continuous moments are used. Furthermore, the method is suggested for highly exact calculation of QDRKMs in polar coordinates where the kernel is thoroughly calculated by over circular color pixels. The translation, scaling, and rotation (TSR) invariances for QDRKMs are demonstrated. Theoretical analysis and numerical experiments investigation were shown in terms of the description performance of TSR invariances, classification, robustness to different noises, and computational times CPU of the QDRKMs compared with continuous quaternion Legendre–Fourier moments using COIL 100 data base.

This work is organized as follows: Section 2 introduces Quaternion Radial Krawtchouk moments (QRKMs). In Sec. 3, the computations of the Quaternion Radial Krawtchouk Moments are calculated. In Sec. 4, a color image reconstruction uses QRKMs. Section 5 takes into account Quaternion Radial Krawtchouk Moments Invariants (QRKMIs) of a test color image for different orders of reconstruction. Section 6 describes the training multilayer perceptron. Some experimental results are presented in Sec. 7, where an evaluation of accurate and computation through some color images have been used. Finally, the conclusions of this research are seen in Sec. 8.

2 Computation of the quaternion radial Krawtchouk moments

2.1 Recurrence relation of Krawtchouk polynomials

The Hyper geometric Krawtchouk polynomial is defined as.

$$k_n(r,p|N) = {}_2F_1\begin{pmatrix} -n, -r \\ -N \end{pmatrix} | \frac{1}{p}); n = 0, 1, 2 \dots N-1; r = N|2; N > 0; p \in (0,1) \qquad (1)$$

Where the orthogonal property of normalized orthogonal polynomial can be rewritten as.

$$\sum_{r=0}^{v-1} \overline{k}_n(r,p|N)\overline{k}_m(r,p|N) = \sum_{k=0}^{\infty} \frac{(-n)_k(-x)_k \left(\frac{1}{p}\right)^k}{(1-N)_{k^{k!}}} = \delta_{nm}; \quad (a)_k$$

$$= a(a+1)(a+2)\dots(a+k-1) \qquad (2)$$

with $(a)_k$ is the Pochhammer symbol and δ_{nm} denote the Dirac function; therefore, the three term recursive relation for the weighted Krawtchouk polynomials is given by.

$$\bar{k}_{n+1}(r,p|N) = \frac{A \times (p \times N + 2pn + n - r)}{p \times (N-n)} \bar{k}_n(r,p|N) - \frac{B \times n(1-p)}{p \times (N-n)} \times \bar{k}_{n-1}(r,p|N); \quad (3)$$

$$for \ n = 0, 1, 2, \dots, N-1$$

Where.

$$A = \sqrt{\frac{p(N-n)}{(n+1)(1-p)}}, \qquad B = \sqrt{\frac{p^2(N-n)(N+1-n)}{(1-p)^2(n+1)_n}}$$

with $n \geq 2$ and the first orders of discrete weighted Krawtchouk polynomials are defined as.

$$\bar{k}_0(r,p|N) = \sqrt{w(0;p,N)}, \quad \bar{k}_1(r,p|N) = \left(1 - \frac{r}{pN}\right)\sqrt{w(0;p,N)}$$

$$w(r+1;p,N) = \left(\frac{N-r}{r+1}\right)\frac{p}{1-p}w(r;p,N), w(0;p,N) = (1-p)^N = e^{N \ln(1-p)} \tag{4}$$

where

2.2 Proposed computations of quaternion radial Krawtchouk moments

The radial Krawtchouk Moments can be rewritten as.

$$
\begin{aligned}
K_{nm} &= \frac{1}{6N} \sum_{r=0}^{N/2} \sum_{\theta=0}^{6N} \bar{k}_n(r,p|N) f(r,\theta) e^{\mu m \theta} \\
&= \frac{1}{6N} \sum_{r=0}^{N/2} \sum_{\theta=0}^{6N} \bar{k}_n(r,p|N) \left(f_R(r,\theta) i + f_G(r,\theta) j + f_B(r,\theta) k \right) e^{\mu m \theta} \\
&= \frac{1}{6N} \left[i \sum_{r=0}^{N/2} \sum_{\theta=0}^{6N} f_R(r,\theta) \bar{k}_n(r,p|N) e^{\mu m \theta} + j \sum_{r=0}^{N/2} \sum_{\theta=0}^{6N} f_G(r,\theta) \bar{k}_n(r,p|N) e^{\mu m \theta} + k \sum_{r=0}^{N/2} \sum_{\theta=0}^{6N} f_B(r,\theta) \bar{k}_n(r,p|N) e^{\mu m \theta} \right]
\end{aligned}
\tag{5}
$$

Where

$$\sum_{r=0}^{N/2} \sum_{\theta=0}^{6N} f(r,\theta) \bar{k}_n(r,p|N) e^{\mu m \theta} = \sum_{r=0}^{N/2} \sum_{\theta=0}^{6N} f(r,\theta) \bar{k}_n(r,p|N) \left(\cos(m\theta) + \frac{i+j+k}{\sqrt{3}} \sin(m\theta) \right)$$

Taking into consideration the proposed value for the quaternion μ, The QRKMs of an RGB image in polar pixels are given by

$$
\widehat{K}_{nm} = \frac{1}{6N} \left[i \left\{ \text{Re}[K_{nm}(f_R)] + \frac{i+j+k}{\sqrt{3}} \text{Im}[K_{nm}(f_R)] \right\} + j \left\{ \text{Re}[K_{nm}(f_G)] + \frac{i+j+k}{\sqrt{3}} \text{Im}[K_{nm}(f_G)] \right\} \right.
$$
$$
\left. + k \left\{ \text{Re}[K_{nm}(f_B)] + \frac{i+j+k}{\sqrt{3}} \text{Im}[K_{nm}(f_B)] \right\} \right]
\tag{6}
$$

Finally,

$$\widehat{K}_{nm} = A_{nm} + i B_{nm} + C_{nm} + k D_{nm} \tag{7}$$

Where,

$$
\begin{aligned}
A_{nm} &= -\frac{1}{\sqrt{3}}\{\mathrm{Im}[K_{nm}(f_R)] + \mathrm{Im}[K_{nm}(f_G)] + \mathrm{Im}[K_{nm}(f_B)]\} \\
B_{nm} &= \mathrm{Re}[K_{nm}(f_R)] + \frac{1}{\sqrt{3}}\{\mathrm{Im}[K_{nm}(f_G)] - \mathrm{Im}[K_{nm}(f_B)]\} \\
C_{nm} &= \mathrm{Re}[K_{nm}(f_G)] + \frac{1}{\sqrt{3}}\{\mathrm{Im}[K_{nm}(f_B)] - \mathrm{Im}[K_{nm}(f_R)]\} \\
D_{nm} &= \mathrm{Re}[K_{nm}(f_B)] + \frac{1}{\sqrt{3}}\{\mathrm{Im}[K_{nm}(f_R)] - \mathrm{Im}[K_{nm}(f_G)]\}
\end{aligned}
\tag{8}
$$

3 Color image reconstruction using QRKMs

The color image $f(r,\theta)$ can be reconstructed using the inverse transformation of QRKMs is given by

$$
\widehat{f}(r,\theta) = \widehat{f}_A(r,\theta) + \widehat{f}_B(r,\theta)i + \widehat{f}_C(r,\theta)j + \widehat{f}_D(r,\theta)k
\tag{9}
$$

With

$$
\begin{aligned}
\widehat{f}_A(r,\theta) &= \mathrm{Re}\left[\widehat{A}(r,\theta)\right] - \frac{1}{\sqrt{3}}\left\{Im\left[\widehat{B}(r,\theta)\right] + Im\left[\widehat{C}(r,\theta)\right] + Im\left[\widehat{D}(r,\theta)\right]\right\} \\
\widehat{f}_B(r,\theta) &= \mathrm{Re}\left[\widehat{B}(r,\theta)\right] + \frac{1}{\sqrt{3}}\left\{Im\left[\widehat{A}(r,\theta)\right] + Im\left[\widehat{C}(r,\theta)\right] - Im\left[\widehat{D}(r,\theta)\right]\right\} \\
\widehat{f}_C(r,\theta) &= \mathrm{Re}\left[\widehat{C}(r,\theta)\right] + \frac{1}{\sqrt{3}}\left\{Im\left[\widehat{A}(r,\theta)\right] - Im\left[\widehat{B}(r,\theta)\right] + Im\left[\widehat{D}(r,\theta)\right]\right\} \\
\widehat{f}_D(r,\theta) &= \mathrm{Re}\left[\widehat{D}(r,\theta)\right] + \frac{1}{\sqrt{3}}\left\{Im\left[\widehat{A}(r,\theta)\right] + Im\left[\widehat{B}(r,\theta)\right] - Im\left[\widehat{C}(r,\theta)\right]\right\}
\end{aligned}
\tag{10}
$$

With

$$
\begin{aligned}
\widehat{A}(r,\theta) &= \sum_{n=0}^{N/2}\sum_{m}^{6N} A_{nm}\,\overline{k}_n(r,p|N)\,e^{\mu m\theta}, \quad \widehat{B}(r,\theta) = \sum_{n=0}^{N/2}\sum_{m}^{6N} B_{nm}\,\overline{k}_n(r,p|N)\,e^{\mu m\theta} \\
\widehat{C}(r,\theta) &= \sum_{n=0}^{N/2}\sum_{m}^{6N} C_{nm}\,\overline{k}_n(r,p|N)\,e^{\mu m\theta}, \quad \widehat{D}(r,\theta) = \sum_{n=0}^{N/2}\sum_{m}^{6N} D_{nm}\,\overline{k}_n(r,p|N)e^{\mu m\theta}
\end{aligned}
\tag{11}
$$

Note that $\widehat{f}_B(r,\theta)$, $\widehat{f}_C(r,\theta)$ and $\widehat{f}_D(r,\theta)$ represent the red, green, and blue color of the reconstructed image, respectively, and L is the maximum order of QRKMIs used in the reconstruction. Typically, the reconstruction formula has been used to recover the image information up to a certain level of approximation.

The difference between the original image and the reconstructed image is measured using the mean squared error (MSE).Which is defined as follows:

$$
MSE = \sum_{r=0}^{N/2}\sum_{\theta=0}^{6N}\left|f(r,\theta) - \widehat{f}\left(r,\theta\right)\right|
\tag{12}
$$

Where $f(r, \theta)$ represents the original color image vector and $\widehat{f}(r, \theta)$ the reconstructed color image.

4 Quaternion radial Krawtchouk moments invariants

In this section, we show a rotation, scaling and translation invariance of Quaternion Radial Krawtchouk Moments invariants (QRKMIs) from [2].

For this, we will them show the invariant moment to be linear combination as well as radial complex moment.

The translation invariance of QRKMs can be easily achieved by transforming the 2D color image to the geometric centre before the calculation of QRKMs. In spite of the scaling and rotation invariance which can be achieved then replacing complex moments, with the 2D complex moment invariants due to Quaternion Radial Krawtchouk moments invariants can be expressed as linear combination of 2D complex moments. In this subsection, we introduce a new and direct method to derive the scaling and rotation invariance of quaternion radial Krawtchouk moments invariants.

Let $f^{rs}(r, \theta)$ be the scaled, and rotated version of image function $f(r, \theta)$ with the scale factor λ and rotation angle θ_0 we have

$$f^{sr}(r, \theta) = f\left(\frac{r}{\lambda}, \theta + \theta_0\right)$$

According to Eq. (5), the QRKMs of scaled and rotated color image is:

$$K'_{nm} = \frac{1}{6N} \sum_{r'=0}^{\frac{N}{2}} \sum_{\theta'=0}^{6N} f\left(\frac{r}{\lambda}, \theta + \theta_0\right) \overline{k}_n(r, p|N) e^{m\mu\theta} \tag{13}$$

By letting $r' = \frac{r}{\lambda} \theta' = \theta + \theta_0$.

Eq. (13) can be written as

$$K'_{nm} = \frac{1}{6N} \sum_{r'=0}^{N/2} \sum_{\theta'=0}^{6N} f\left(r', \theta'\right) \overline{k}_n(\lambda r', p|N) e^{m\mu\left(\theta'-\theta_0\right)} \tag{14}$$

Where the polynomial of Krawtchouk is defined [38]

$$\overline{k}_n(\lambda r, p|N) = \sum_{i=0}^{n} C(n, i) \lambda^i r^i$$

and

$$C(n, i) = \sum_{k=0}^{n-i} \overline{B}_{n,n-k} s(n-k, i)$$

$$\overline{B}_{n,n-k} = w(r; p, N) B_{n,n-k}$$

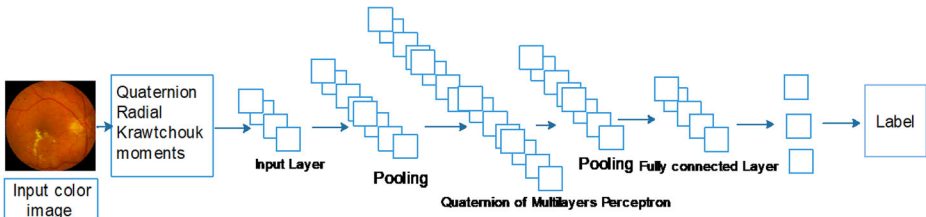$$B_{n,k} = \frac{-1^k n!(N-k)!}{(N-k)!N!k!p^k}$$

Fig. 1 Quaternion Discrete Radial Krawtchouk convolutional neural networks architecture

and $s(n-k,i)$ is the stirling numbers of the first kind, with $s(k, 0) = s(0, i = 0, k \geq 1, i \geq 1)$ and $s(0,0)=1$.

Therefore, the relationship between the original and rotation scaled QRKMs can be formed as

$$\varphi_{nm} = \sum_{k=0}^{n} \sum_{l=0}^{m} \eta_{n,k}\eta_{m,l}K'_{kl} = \lambda^n e^{m\mu\theta_0} \sum_{k=0}^{n} \sum_{l=0}^{m} \eta_{n,k}\eta_{m,l}K_{kl}$$

where

$$\eta_{n,k} = 1 \, (n = k), \eta_{n,k} = \sum_{r=0}^{n-k-1} \frac{-C(n-r,k)\eta_{n,n-r}}{C(k,k)}$$

To eliminate the scale factor, we construct the normalized rotation and scale invariants of QRKMIs

$$\psi_{nm} = \frac{\varphi_{nm}\varphi_{00}^{\gamma+1}}{\varphi_{n+\gamma,0}\varphi_{0,m+\gamma}}, n, m = 0, 1, 2, \ldots, \gamma = 1, 2, 3, \ldots \tag{15}$$

Then, $_{nm}$ is scaling and rotation invariance of QRKMs for any orders n, m.

5 Pattern classification of multi-layer perceptron

5.1 Descriptor vector of color image

These QRKMIs can be used to form the descriptor vector of each color image. Specially that the latter composed of QRKMs up to order S, where S is experimentally selected.

Order	10	20	30	50	80	100
Proposed Method						
NIRE of Proposed Method	0.0093	0.0092	0.0091	0.0046	0.0023	0.00198
NIRE QLFMs[20]	0.0353	0.0176	0.0113	0.0054	0.0026	0.0021

Fig. 2: Reconstructed color image using the proposed method compared with QLFMs. Color test image from (**a**) diabetic retina and (**b**) normal retina, dataset benchmarking diabetic (http://www.it.lut.fi/project/imageret/diaretdb1/).

(a)   (b)

Color test image from (a) diabetic retina and (b) normal retina , dataset benchmarking diabetic [27]

Order	10	20	30	50	80	100
a: p=0.3						
b: p=0.3						
a : p=0.5						
b : p=0.5						
a : p=0.8						
b : p=0.8						
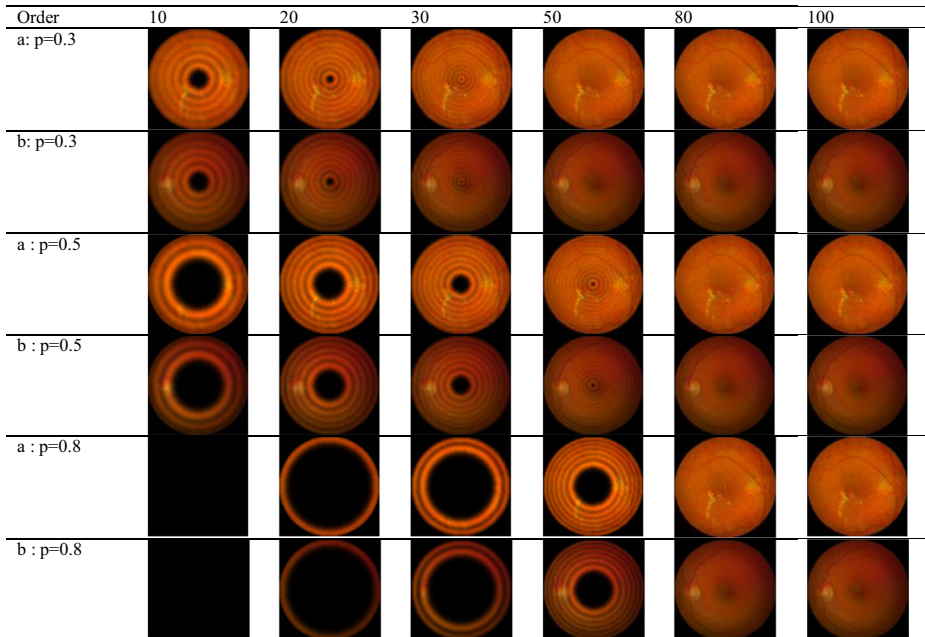
Fig. 3: Reconstructed color image of retina of size 128×128 using the proposed method.

The characteristic vectors V_{2D} is represented as

$$V_{2D\_Color\_Image} = [\psi_{nm} | n + m \in [0, 1, \ldots S]] \qquad (16)$$

To perform the recognition of color image to its appropriate classes. We use multi-layer perceptron from V_{query} and V_{test} where V represent the characteristic vectors $V_{2D\_Color\_Image}$.

where the T-dimensional feature Vquery is represented as

$$V_{query} = \left[V_{query}^1, V_{query}^2, \ldots, V_{query}^T \right] \qquad (17)$$

and the T-dimensional training vector of class K is shown as

$$V_{test}^K = \left[V_{test}^1, V_{test}^2, \ldots, V_{test}^T \right] \qquad (18)$$
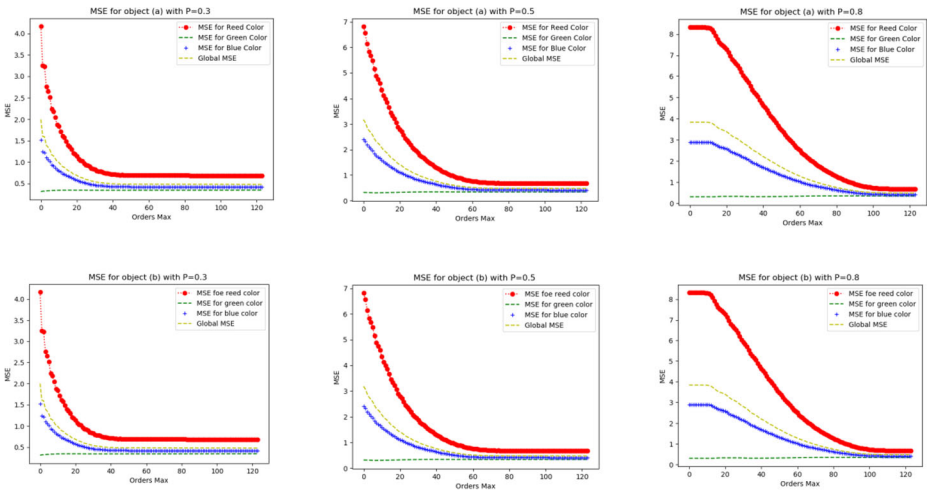
Fig. 4 MSE for Objects (**a**, **b**) with $p = 0.3, 0.5, 0.8$

5.2 Classification of 2D color object using a multi-layer perceptron

The Learning of Multilayer Perceptron MLP is the process to adapt the connection weights. in order to obtain a minimal difference between the network output and the desired output. For this reason in the literature some algorithms are used as an Ant colony, but the most used called Back-propagation which is based on descent gradient techniques. Assuming that we used an input Layer with n_0 neurons $V_{2D\_Color\_Image} = (r_0, r_1, \ldots, r_n)$ and a sigmoid activation function $f(x)$ where

$$f(r) = \frac{1}{1 + e^{-r}} \tag{19}$$

To get the network output, we need to compute the output of each unit in each layer. Now, consider a set of the hidden layers $(h_1, h_2, \ldots, h_N)$, assuming that N_i is the neurons number in each hidden layer h_i.
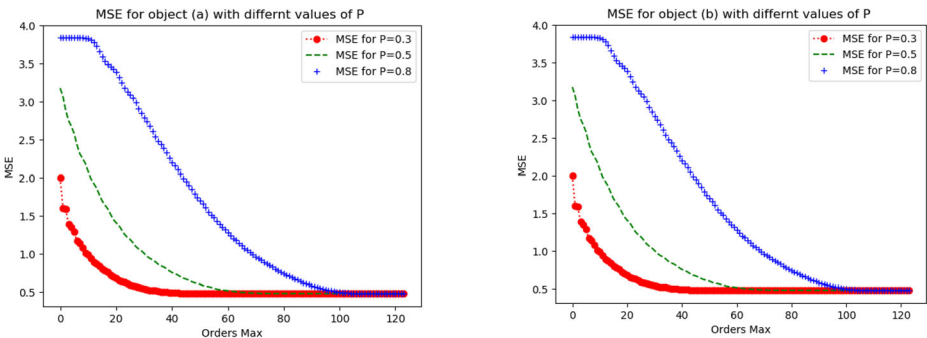

Fig. 5 MSE for objects (**a**, **b**) with different values of p.

Springer

Fig. 6. color image Database Coil-100 (http://www.cs.columbia.edu/CAVE/software/softlib/coil-100.php).

For the output of first hidden layer

$$h_1^i = f\left(\sum_{k=1}^{n_0} w_{kj}^0 x_k\right); j = 1, 2, \ldots, n \tag{20}$$

Let's admit a set of hidden layers ($h_1, h_2, \ldots, h_N$), assuming that n_i is the neurons number in each hidden layer h_i. For the outputs h_i^j of neurons in the hidden layers are calculated as follows:

$$h_i^j = f\left(\sum_{k=0}^{n_{i-1}} w_{kj}^{i-1} h_{i-1}^k\right); i = 2, \ldots, N; j = 1, \ldots, n_i \tag{21}$$

Where w_{kj}^i is the weight between the neuron k in the hidden layer i and the neuron j in the hidden layer $i+1$, n_i is the number of the neurons in the ith hidden layer, The output of the ith layers can be formulated by.

$$h_i = t\left(h_i^1, h_i^2, \ldots \ldots h_i^{n_i}\right) \tag{22}$$

The network outputs are computed by

$$y_i = f\left(\sum_{k=1}^{n_N} w_{kj}^N h_n^k\right); Y = (y1, \ldots \ldots, yi, \ldots \ldots, y_{N+1}) = F(W, X) \tag{23}$$

Where w_{kj}^N is the weight between the neuron k of the Nth hidden layer and the neuron j of the output layer, n is the number of the neurons in the Nth hidden layer, Y is the vector of the output

Original (128x128)   S1 (100x100)   S2 (80x80)   S3 (60x60)   S4 (40x40)

Fig 7 Scaled color images of the obj6 (Coil - 100)

Table 1 Scaling invariances of the scaled images using the proposed method

Scaling Factor	$QRKMI_{1.1}$	$QRKMI_{1.2}$	$QRKMI_{2.1}$	$QRKMI_{2.2}$	$QRKMI_{2.3}$	$QRKMI_{3.2}$
Original (128 × 128)	0,032711399	0,027784444	0,030710125	0,133,626,263	0,024581251	0,03816812
S1 (100 × 100)	0,019466042	0,075414081	0,023994708	0,059765772	0,010332615	0,082692953
S2 (80 × 80)	0,019974595	0,089813706	0,024304697	0,07757921	0,007044542	0,056255515
S3 (60 × 60)	0,013468346	0,023986918	0,009906989	0,043417669	0,008520449	0,059531946
S4 (40 × 40)	0,001546845	0,000811837	0,003828326	0,002414154	0,000404792	0,005697043
σ/μ	0,01131493	0,04750533	0,01127255	0,0703759	0,01202974	0,04501641
Average σ/μ	0,928,139,949					

layer, F is the transfer function and W is the weights matrix, it's defined as follows

$$W = \left[W^0, ..., W^j, ...W^N \right]$$
$$Wi = (w^i_{j,k})_{\substack{0 \leq i \leq N \\ 1 \leq j \leq n_{i+j} \\ 1 \leq k \leq k_{ni}}} \qquad where \quad w^i_{j,k} \in R \tag{24}$$

Where X is the input of neural network and f is the activation function and W^i is the matrix of weights between the ith hidden layer and the $(i + 1)^h$ hidden layer for i= 1, …, $N-$ 1, W^0 is the matrix of weights between the input layer and the first hidden layer, and W^N is the matrix of weights between the Nth hidden layer and the output layer.

The Fig. 1 represent the Quaternion Discrete Radial Krawtchouk convolutional neural networks architecture.

6 Numerical experiments

In this section, we show the reconstruction results obtained using some color test images. These RGB test images are shown in Fig. 2 using Eq. (12), we have reconstructed the three cases of test images.

6.1 Reconstruction results using QRKMs for color images

In this experiment result, the color image reconstruction capability of QRKMs is shown for Lena in Fig. 2 and diabetic retina in Fig.3. Several comparisons of means square error for
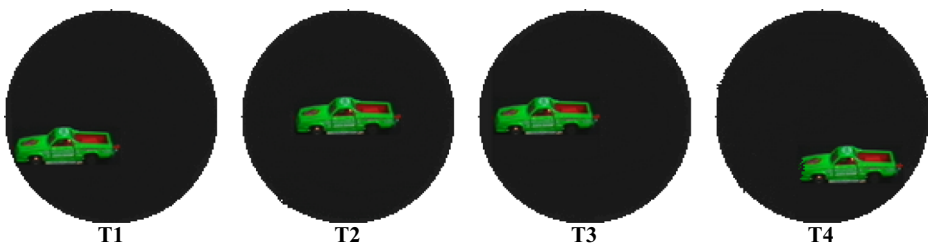

| T1 | T2 | T3 | T4 |

Fig. 8 Translated color object from Coil – 100 database.

Table 2 Translation invariances of the translated images using the proposed method

Translated images	$QRKMI_{1.1}$	$QRKMI_{1.2}$	$QRKMI_{2.1}$	$QRKMI_{2.2}$	$QRKMI_{2.3}$	$QRKMI_{3.2}$
T1	0,01098284	0,00571108	0,02034120	0,00352828	0,00683267	0,01057263
T2	0,00435062	0,01763953	0,00589206	0,02845574	0,00453517	0,03454778
T3	0,02089574	0,02430416	0,02581992	0,02635603	0,01988594	0,02527690
T4	0,00290669	0,0375715	0,00791073	0,01539686	0,00596872	0,00771857
σ/μ	0,72,583,313	0,54,035,151	0,55,692,289	0,53,879,406	0,66,233,221	0,55,994,206
Average σ/μ			0,597,362,645			

different parameters of QRKMs in Figs.4 and 5 and the comparison with QLFMs is also given in this part. We use the statistical computation of normalization image reconstruction error to measure the performance of the color image reconstruction, we deduce that the QRKMs are more convenient instead of QLFMs .

The means square Error (MSE) (Fig. 5) for color image has been usually used to describe how well a color image can be retrieved by a small and big set of QRKMs.

6.2 Invariability for QRKMs

To validate the invariability for QRKMs of the QRKMIs, we use some objects from Coil-100 Database Fig. 6.

The selected order of the invariants ($QRKMIs_{00}$; $QRKMIs_{12}$; $QRKMIs_{22}$; $QRKMIs_{23}$, $QRKMIs_{32}$) are computed for each image. The results of simulation the scaling invariances of color image Fig.7 are shown in Table 1, the translation invariances of color image Fig.8 are shown in Table 2, the rotation invariances of color image Fig. 9 are shown in Table 3. Finally, the ratio σ/μ can use to measure the capability of the proposed QRKMIs under different image transformation, where σ represents the standard deviation of QRKMs the different factors of each rotation, and μ is the equivalent mean value. The Table 1, 2 and 3 show that the ratio σ/μ is very low and consequently the QRKMIs are very stable under different types of color image Figs. 7, 8 and 9. Hence, the property of invariability of QRKMIs will be used to pattern classification.

7 Classification the color image using QRKMs

In this subsection, we will discuss the classification the color image using QRKMs.

To validate the proposed approach for classification, we have taken the color image from the **benchmarking diabetic dataset** [32]. The total number of color images is 2

Fig. 9 Rotated color object from Coil – 100 database.

Table 3 Rotation invariances of the rotated images using the proposed method

| rotated images	$QRKMI_{1.1}$	$QRKMI_{1,2}$	$QRKMI_{2,1}$	$QRKMI_{2,2}$	$QRKMI_{2,3}$	$QRKMI_{3,2}$
Original	0.0256747228217753	0.0346922022334480	0.023342188257925	0.1330912118283 88	0.0155593267 5581	0.0105769356771 75
$\alpha = 10°$	0.0223971151357427	0.029198658412736	0.018660392151952	0.11185143683 6449	0.0115707829 6405	0.012310519123945
$\alpha = 60°$	0.0114075567611123	0.032259007875538	0.015489410648314	0.124182129234384	0.0120696503 1292	0.017242479424019
$\alpha = 80°$	0.0167279373904 0	0.035805799092379	0.018550670775727	0.13511612057 5067	0.0184003368 2210	0.0153412599 56574
$\alpha = 120°$	0.0312759810509 5	0.010469983695349	0.028142803340050	0.036319678888727	0.0163392316 97028	0.0237194267 47404
σ/μ	0,35,915,502	0,45,624,667	0,24,042,125	0,97,331,196	0,54,396,651	0,5,134,797
Average σ/μ			0,514,430,184			
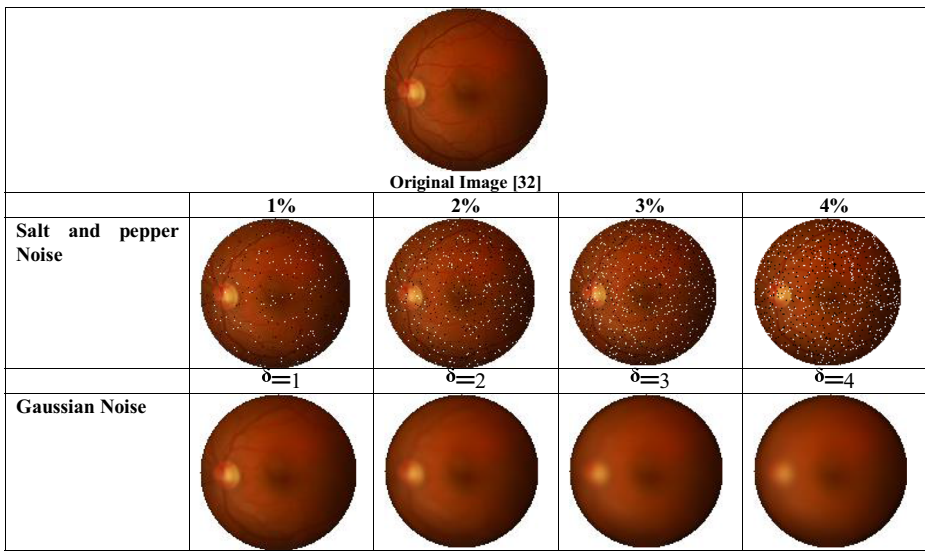
Fig. 10: Computation of Salt and Pepper Noise & Gaussian Noise for color image.

distributed as 89 images for each object. All color images of this database have the size 128×128 (after adaptation). The test set also degraded by Gaussian and salt and pepper noise with noise densities 1%, 2%, 3%, and 4%. Figure 10 show the densities of Salt and Pepper Noise & Gaussian Noise for color image. The feature vector based on QRKMIs is use to classify these images and its recognition accuracy is compared with that of quaternion Legendre–Fourier momentsThe results of the classification using all features are presented in Table 4.

8 Conclusion

In this paper, we suggested a new method to calculate the Quaternion Radial Krawtchouk moments, we have also proposed a classification of multi-layer perceptron of Quaternion Radial Krawtchouk moments. The performances of the proposed Quaternion Radial Krawtchouk moments invariants have been tested under different color images. The results obtained show that the representation capability is compared with different color of the same image. This proposed approach has been significantly improved by using the multi-layer perceptron for classification of Quaternion Radial Krawtchouk moments and can highly be useful in the field of color image analysis, and the test of color images are

Table 4 Classification results of Princeton Shape Benchmark (PSB) using Multi-Layer Perceptron

Invariant moments	Noise-free	Salt and pepper noise			
		1%	2%	3%	4%
Quaternion Legendre–Fourier	100%	89,61%	86,25%	80,97%	61,36%
Proposed method	100%	93,25%	90,32%	85,35%	69,03%

clearly classified from a set of images that are available in benchmarking diabetic dataset for color image.

References

1. Amakdouf H, El Mallahi M, Zouhri A, Qjidaa H (2018) Classification and recognition of 3D image of charlier moments using a multilayer perceptron architecture. Procedia Computer Science 127(2018):226–235

2. Cao L, Zhi R, Jin Y (2018) Translation and scale invariants of krawtchouk moments. Inf Process Lett 130(C):30–35

3. Chen B, Shu H, Zhang H, Chen G, Luo L (2010) Color image analysis by quaternion zernike moments. In: Proceedings - international conference on pattern recognition

4. Chen BJ, Shu HZ, Zhang H, Chen G, Toumoulin C, Dillenseger JL, Luo LM (2012) Quaternion Zernike moments and their invariants for color image analysis and object recognition. Signal Process 92:308–318. https://doi.org/10.1016/j.sigpro.2011.07.018

5. Chen B, Shu H, Coatrieux G, Chen G, Sun X, Coatrieux JL (2014) Color image analysis by quaternion-type moments. J Math Imaging Vis

6. Chen B, Qi X, Sun X, Shi YQ (2017) Quaternion pseudo-Zernike moments combining both of RGB information and depth information for color image splicing detection. J Vis Commun Image Represent 49: 283–290. https://doi.org/10.1016/j.jvcir.2017.08.011

7. El Mallahi M, Mesbah A, El Fadili H, Zenkouar K, and Qjidaa H. (2014) Compact computation of krawtchouk moments for 3D object representation. *WSEAS transactions on circuits and systems* E-ISSN: 2224-266X,13.

8. El Mallahi M, Mesbah A, El Fadili H, Zenkouar K, et H. Qjidaa. (2015) Translation and scale invariants of three-dimensional Krawtchouk moments, IEEE 2015 intelligent systems and computer vision, ISCV .

9. El Mallahi M, Mesbah A, Qjidaa H. (2016). "An algorithm for fast computation of 3D Krawtchouk moments for volumetric image reconstruction", Proceedings of the Mediterranean Conference on Information & Communication Technologies 2015 pp 267-276

10. El Mallahi M, Mesbah A, El Fadili H, Zenkouar K, et Qjidaa H (2016) "Volumetric image reconstruction by 3D hahn moments." 2015 ieee/acs 12th international conference of computer systems and applications (AICCSA).

11. El Mallahi M, Mesbah A, Qjidaa H (2016) "Fast algorithm for 3D local feature extraction using Hahn and Charlier moments" advances in ubiquitous networking 2, Lecture notes in electrical engineering, vol 397. Springer, Singapore

12. El Mallahi M, Zouhri A, EL-mekkaoui J, Qjidaa H (2017) Three dimensional radial Krawtchouk moment invariants for volumetric image recognition. Pattern Recognit Image Anal 27(4):810–824

13. El Mallahi, M. et al. (2017) 'Three dimensional radial tchebichef moment invariants for volumetric image recognition', Pattern Recognition and Image Analysis

14. El Mallahi M, Zouhri A, Mekkaoui J and Qjidaa H (2017) "Radial Meixner moments for rotational invariant pattern recognition", IEEE 2017 intelligent systems and computer vision, ISCV .

15. El Mallahi, M. et al. (2017) Radial charlier moment invariants for 2D object/image recognition, in international conference on multimedia computing and systems -proceedings

16. El Mallahi M, Zouhri A, Amakdouf H, Qjidaa H (2018) Rotation scaling and translation invariants of 3D radial shifted Legendre moments. Springer, International Journal of Automation and Computing, Springer, April 2018 15(2):169–180

17. M. El Mallahi, A. Mesbah, et H. Qjidaa. (2018)."3D radial invariant of dual hahn moments." Springer, Neural Computing and Applications. , Vol. 30, Issue 7, pp 2283–22.

18. El Mallahi M, Zouhri A, Mesbah A, El Affar I, Qjidaa H (2018) Radial invariant of 2D and 3D Racah moments. Springer, Multimedia Tools and Applications An International Journal 77(6):6583–6604

19. Mesbah A, El Mallahi M, Qjidaa H (2016) "Fast and efficient computation of three-dimensional Hahn moments" SPIE. Journal of electronic imaging 25(6):061621
20. Mesbah A, Zouhri A, El Mallahi M, Qjidaa H. (2017)."Robust reconstruction and generalized dual hahn moments invariants extraction for 3d images" spriger, 3D Research Center, Kwangwoon University and Springer-Verlag Berlin Heidelberg, vol. 8, num. 7, Issues 29
21. Mukundan, R. (2012) 'A comparative analysis of radial-Tchebichef moments and Zernike moments', in. doi: https://doi.org/10.5244/c.23.16.
22. Wang XY, Li WY, Yang HY, Wang P, Li YW (2015) Quaternion polar complex exponential transform for invariant color image description. Appl Math Comput 256:951–967. https://doi.org/10.1016/j.amc.2015.01.075
23. Xiang-Yang W, Wei-Yi L, Hong-Ying Y, Pan-Pan N, Yong-Wei L (2015) Invariant quaternion radial harmonic Fourier moments for color image retrieval. Opt Laser Technol 66:78–88. https://doi.org/10.1016/j.optlastec.2014.07.020
24. Xiao B, Ma JF, Cui JT (2012) Radial Tchebichef moment invariants for image recognition. J Vis Commun Image Represent 23:381–386
25. Xiao B, Wang GY, and Li WS (2014) Radial shifted legendre moments for image analysis and invariant image recognition Image Vis. Comput.
26. Xiao B, Zhang Y, Li L, Weisheng L, Wang G (2016) Explicit Krawtchouk moment invariants for invariant image recognition. J Electron Imaging 25(2):023002